

# Synthesis and Studies of Digital Frequency Modulator-demodulator with Non-Coherent Demodulator Containing a Band-pass Active Filter

B. Karapenev

Technical University of Gabrovo, Bulgaria

Department of the Communication Equipment and Technologies

bkarapenev@tugab.bg

**Abstract**— This paper presents a scientific- and practically-applied development of the digital frequency modulator-demodulator. This includes a conceptual project, synthesis and the design of its main blocks: non-coherent digital frequency demodulator containing a band-pass active filter and an amplitude detector. Results of the carried out simulation and experimental studies of developed laboratory model were presented. The paper presents a synthesis of a digital frequency demodulator model without the use of specialized components and integrated circuits available in the libraries of simulation study software. This is possible by choosing a non-coherent circuit variant. Results of the simulation and experiments indicated that the synthesis, design and modeling of the non-coherent FSK demodulator was successful.

**Index Terms**— Band-pass Active Filter; Demodulator; Digital Frequency Modulator; Non-coherent; Studies; Synthesis.

## I. INTRODUCTION

The transmission of information at long distances is related to the use of modulation and demodulation processes and corresponding devices - modulators and demodulators. Initially, the amplitude, frequency and phase analog modulators/demodulators have found a wide application in practice [1]. The improvement of communication systems in recent years has led to their digitalization of the input information signals, their method of processing and their transmission over the communication channel.

The block diagram of a communication system is shown in Figure 1. The transmitter, receiver and transmission environment form the so-called radio channel or connection channel. Modulators and demodulators are nonlinear devices that in modern duplex communication systems often merge and form a common module – MoDem [2].

The modulation signal in digital modulation  $u_{\Omega}(t)$  is a numerical series of logical 0 and logical 1, and the carrier oscillation is sinusoidal and has the following form:

$$u_H(t) = U_{Hm} \sin(\omega_H t + \varphi_H). \quad (1)$$

The carrier oscillation parameters in the modulation process change by jumping between two states defined by the digital signal: logical 0 or logical 1. Thus, the amplitude, frequency and phase of the carrier oscillation receive discrete values in tact with the modulating digital series. The main types of digital manipulations are: Amplitude Shift Keying – ASK, Frequency Shift Keying – FSK, Phase Shift

Keying – PSK and Quadrature-Amplitude Modulation – QAM, which are of higher degree.

The modulated signal in frequency manipulation (FSK) is formed as the sum of two ASK signals, each with the corresponding carrier frequency  $f_{C1}$  and  $f_{C2}$ .

The mathematical model of the modulated FSK signal has the following form:

$$u_{FSK}(t) = A \cdot \sin(2\pi f_{C1} t) + A \sin(2\pi f_{C2} t). \quad (2)$$

Its functions are binary and it accepts only two values - logical 0 or logical 1.

## II. SYNTHESIS OF DIGITAL FREQUENCY MODULATOR-DEMODULATOR - A CONCEPTUAL DESIGN

The transmitted information from the signal source to the receiver to be transferred over a communication channel requires it to be modulated, and accordingly demodulated [3]. The digital frequency modulator-demodulator performs the function of signal formation, their transmission - transfer over the communication channel and their reception. The connection channel may be a cable or ethereal (terrestrial, satellite) [4].

The block diagram of a digital frequency modulator-demodulator is shown in Figure 2. The input digital signal in the FSK modulator, the information carrier, is converted to a continuous one, which is transmitted over an analogue connection channel. It is characterized by the following more important parameters and characteristics: Signal-to-Noise Ratio (SNR) and linearity of amplitude and phase responses. The input continuous signal in the FSK demodulator is converted into an output digital signal carrier of the information.

The FSK modulator can be implemented on the basis of various circuit solutions, such as using the widely distributed module-timer 555 or Schmitt-trigger comparator using different capacities to provide a different frequency of output signal.

In order to ignore the influence of the communication channel, it is assumed that the channel is ideal – i.e. there is a direct connection between the FSK modulator and the demodulator.

The FSK demodulator can be [2]:

- built on the basis of a non-coherent scheme, in which direct frequency demodulation of the oscillations is performed;

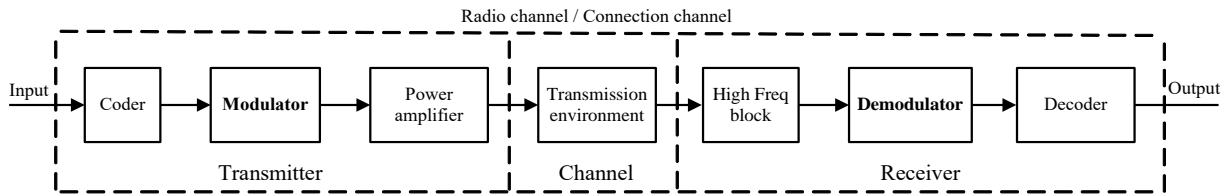


Figure 1: The block diagram of a communication system

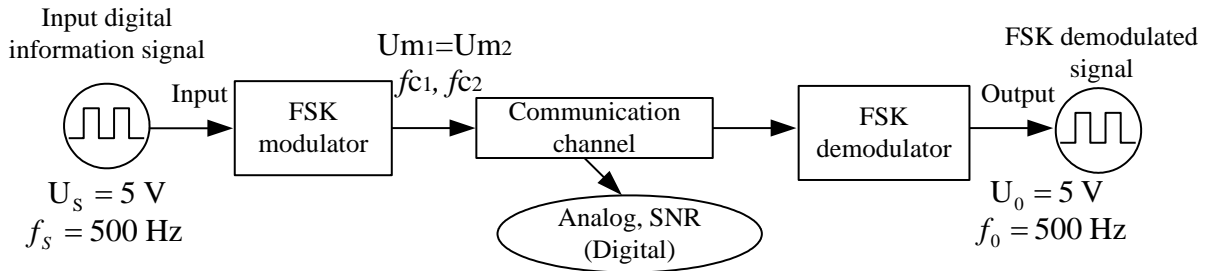


Figure 2: Block diagram of digital frequency modulator-demodulator

- differential-coherent, in which the digital series is differentially encoded before performing the frequency manipulation;
- coherent, where synchronous demodulation is performed using an automatic frequency adjustment system. In this case, a specialized PLL or FPGA [5] integrated circuits (IC) is used;
- implemented with a Digital Signal Processor (DSP).

The implementation of a FSK demodulator with discrete elements, i.e. without the use of specialized IC, DSP and processors, can only be done through a non-coherent scheme [6]. Circuit of a non-coherent FSK demodulator can be synthesized based on the block diagrams, showed in Figure 3 and Figure 4 [7].

Non-coherent demodulation of binary FSK modulated signals can be performed by frequency discrimination as shown in Figure 3. Two parallel-connected circuits transmit one of the two frequencies  $f_{c1}$  and  $f_{c2}$  and form the amplitudes of the signals from the demodulation performed. The output digital frequency demodulated signal is formed by comparing the two  $U_{m1}(t)$  and  $U_{m2}(t)$  signals, which can be performed by a comparator.

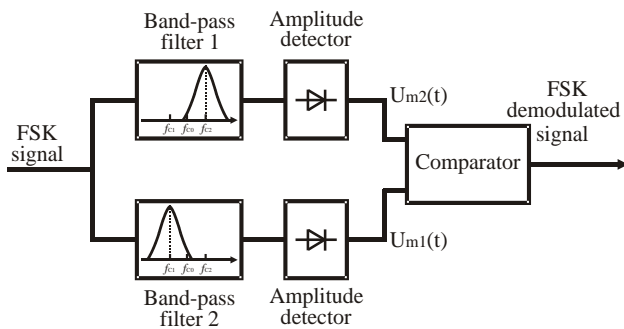


Figure 3: Block diagram of non-coherent digital frequency demodulator

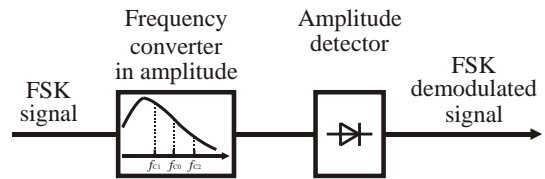


Figure 4: An non-coherent digital frequency demodulator

The block diagram of the non-coherent FSK demodulator of Figure 4 consists of a converter of frequency into amplitude and an amplitude detector. The two frequencies  $f_{c1}$  and  $f_{c2}$  are in the fall of the amplitude-frequency response (AFR) of low-pass filter or the rising or falling slope of the AFR of band-pass filter for which the voltage transmission coefficient is different. This process is illustrated with the timing diagrams shown in Figure 5 [7].

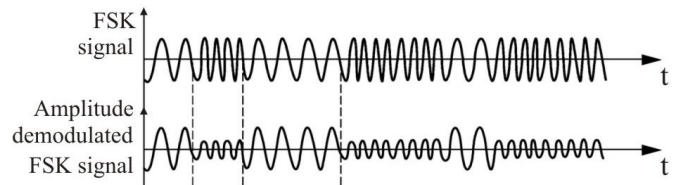


Figure 5: Time-diagrams of the amplitude-demodulated FSK signal

In the non-coherent FSK demodulator (Figure 4), two identical series-connected units of band-pass active filters (BPAF) were used as frequency/amplitude converter. It was done in order to provide the corresponding voltage transmission coefficients in the course of the AFR for frequencies  $f_{c1}$  and  $f_{c2}$ . For this purpose, both the increasing and decreasing slopes of the AFR can be used. The output amplitude-demodulated signals should be submitted to a voltage comparator with positive feedback and a hysteresis zone of its switching  $U_x$ , and the input digital modulation signal carrier of the information appears at the output.

The choice of the drop in the amplitude-frequency response of the BPAF used is of great importance. The analytical expression of the transfer function (AFR) for polynomials BPAF is of the type [8]

$$T_B(s) = \frac{U_{out}}{U_{in}} = \frac{H_0 \cdot s^{n/2}}{s^n + b_{n-1}s^{n-1} + \dots + b_1s + b_0}, \quad (3)$$

where  $U_{out}$  and  $U_{in}$  are respectively the output and input voltages,  $s = j\omega$  is the complex variable, and  $n$  is the order of the filter and can accept a random even number. The steepness of the drop of the AFR outside the over speed frequency band is determined by the order of the filter  $n$ . The transmission coefficient  $H_0$  does not depend on the type of BPAF, but on its schematic implementation and is involved in determining the transmission coefficient  $T_0$  of the band-pass filter in the bandwidth. The coefficients  $b_i$  in the denominator depend on the type of BPAF, i.e. they have different values in polynomial BPAF with Butterworth and Chebychev approximation.

The transmission function (3) can be presented as a product of second order multipliers, used in the implementation of narrowband BPAF, and has the type

$$T_B(s) = \frac{U_{out}}{U_{in}} = \frac{H_{01} \cdot s}{s^2 + b_{11}s + b_{01}} \cdot \dots \cdot \frac{H_{0m} \cdot s}{s^2 + b_{1m}s + b_{0m}}, \quad (4)$$

or the BPAF contains  $m$  number of band-pass units of second order.

As units of second order BPAF can be used:

- broadband units with polar Q-factor  $< 0,5$  and  $H_{0max} < 1$ ;
- band-pass units with polar Q-factor  $\leq 10$ ;
- band-pass units with polar Q-factor from 10 to 100;
- band-pass units with polar Q-factor from 100 to 500.

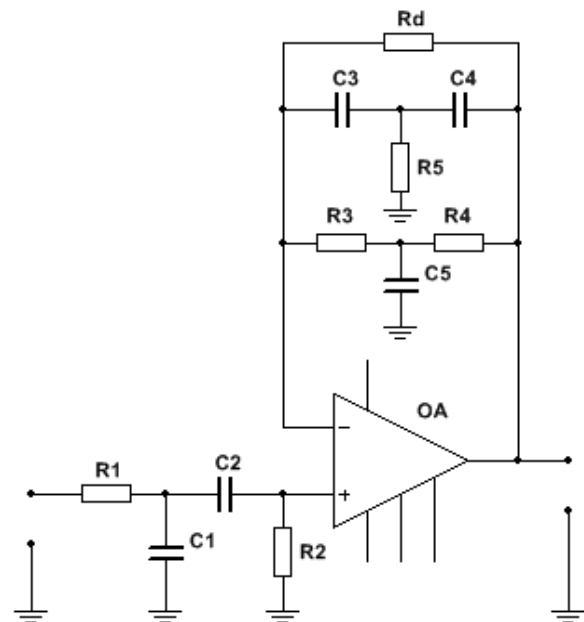
The last mentioned units were built using three operational amplifiers (OA) as the first one is connected as a two-input adder, and the second and the third - as multipliers whose transmission coefficient depends on the frequency.

The schematic variant in Figure 6 is chosen from the listed possible variants of band-pass active units for the implementation of BPAF from the structure of the FSK demodulator. It has a comparatively high quality factor and a high transmission coefficient of the center frequency  $T_0$ .

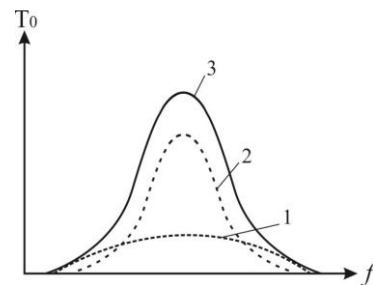
The circuit of a band-pass unit with a polar Q-factor from 10 to 40 is shown in Figure 6a [8]. The transmission coefficient for the average frequency of the unit is approximately equal to  $(3.4Q)$ . A two-unit passive band-pass RC filter is connected between the input of the unit and the non-inverting input of the OA (resistors  $R_1$ - $R_2$  and capacitors  $C_1$ - $C_2$ ) but in the negative feedback chain – a bridged symmetrical double T-bridge is connected. If the negative feedback chain is frequency-independent, then the AFR of the whole unit is determined by the two-unit passive band-pass filter - Figure 6b curve 1. When connecting only the bridged double T-bridge in the negative feedback chain, the unit has an AFR with higher selectivity and a higher maximum transmission coefficient - curve 2. This is due to the fact that the transmission coefficient of the double T-bridge itself has a minimum at a given frequency for which the depth of negative feedback is the smallest, and the transmission coefficient of the unit is maximum. In the joint action of the two-unit passive RC filter and the double T-bridge, an AFR is obtained with a much greater selectivity and maximum transmission coefficient in the bandwidth - curve 3.

The main advantages of the circuit are the presence of only one OA and the good manufacturability due to the large number of passive elements with the same values.

In the exchange of the elements  $C_2$  and  $R_2$ , a polynomial low-frequency unit of second order with a polar Q-factor from 10 to 50 is realized, whose decrease of the AFR in the high-frequency can also be used as a frequency converter into amplitude.



(a)



(b)

Figure 6: A band-pass unit of II order with Q from 10 to 40 (a) - simplified circuit; (b) - AFR of the component circuits

### III. DESIGN OF DIGITAL FREQUENCY MODULATOR-DEMODULATOR AND SIMULATION RESULTS

Design and studies of digital frequency modulators - using Module-timer 555 and Schmitt-trigger are presented in [9] and [10] respectively.

#### A. Design of the one Band-pass Active Filter Unit from the Structure of the Digital Frequency Demodulator

The set of output data for the design of a single unit of BPAF from the structure of the digital frequency demodulator are as follows:

- order of the unit - second;
- a maximum center frequency  $f_C = 1$  kHz;
- a free term in the denominator of the transmission function  $b_{0B} = 3.3137$ ;

- coefficient in front of the complex variable ( $s$ ) in the denominator of the transmission function  $b_{1B} = 2.3722$ .

The choice of the order  $n$  of the Chebychev approximation filter was performed by a nomogram, as the set normalized frequency  $\Omega_a$ , the transmission coefficient  $T$  and the unevenness  $\Delta a$  in the bandwidth were determined.

The number of filter units, the value of the coefficients  $b_{0B}$  and  $b_{1B}$  of their transmission functions and the polar Q-factor were taken from a table to determine the coefficients by detecting the order of the filter and the unevenness  $\Delta a$ .

The capacity  $C$  was chosen and the values of the remaining passive elements were calculated by [8]:

- the capacitances were chosen -  $C_1 = C_2 = C = 10$  nF;
- the help factor for the ratio of the resistances in unit  $d$  was determined by:

$$d = \frac{1 + \sqrt{1 + 4 \cdot b_{0B} / b_{1B}^2}}{4 \cdot \frac{b_{0B}}{b_{1B}^2}} = 1.2023534; \quad (5)$$

- resistances  $R_1$  and  $R_2$  were determined by:

$$R_4 = R_5 = R = \frac{d}{\pi \cdot f_C \cdot b_{1B} \cdot C} \approx 16 \text{ k}\Omega; \quad (6)$$

$$R_1 = \frac{R}{2 + d + \sqrt{2 + d^2}} \approx 3.2 \text{ k}\Omega; \quad (7)$$

$$R_2 = \frac{R^2}{(1 + 2 \cdot d) \cdot R_1} \approx 24 \text{ k}\Omega; \quad (8)$$

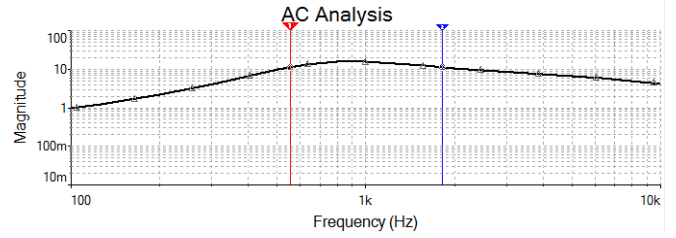
- resistances  $R/2$  and  $R/d$  were also determined as well as the capacitance  $2 \cdot C$

$$R_3 = \frac{R}{d} \approx 13 \text{ k}\Omega; \quad R_6 = \frac{R}{2} \approx 8 \text{ k}\Omega; \quad (9)$$

$$C_5 = 2 \cdot C = 20 \text{ nF}. \quad (10)$$

For the one and two units of BPAF of the structure of the non-coherent digital frequency demodulator, which has the function of a frequency converter in amplitude, simulation studies were performed with the MultiSIM module of the Circuit Design Suite package. The parameters of the input signal from the Functional generator are: Amplitude 5 V, Frequency 0.5 kHz, sinusoidal signal form and signal Offset 5 V, so that the submitted input signal of the filter can be analogous to the one received by the digital frequency modulator.

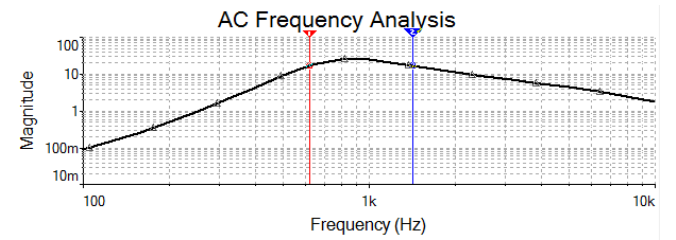
The obtained AFR of the BPAF with one and two units of the performed AC Frequency Analysis are presented in Figure 7 and Figure 8 respectively. Their realized main parameters are also indicated: A maximum transmission coefficient  $T_0$ , below-  $f_B$  and high-  $f_H$  cut-off frequency and missed bandwidth  $\Delta f$ .



$$T_0=3.16, f_B=555\text{Hz}, f_H=1820\text{Hz}, \Delta f=1265\text{Hz}$$

Figure 7: AFR of one unit of BPAF

The results obtained for one and two BPAF units are identical because the units are non-inverting for the operating frequencies  $f_0$  and  $f_1$ . The maximum transmission coefficient for the center frequency is one and the same  $f_C = 800$  Hz in both cases. The frequency, at which there is no phase difference between the output and the input signal, is:



$$T_0=5, f_B=620\text{Hz}, f_H=1420\text{Hz}, \Delta f=800\text{Hz}$$

Figure 8: AFR of two units of BPAF

the same  $f = 1200$  Hz. The selectivity of the two-unit BPAF is greater, as in the case of a missed frequency bandwidth  $\Delta f = 800$  Hz, but the total harmonic distortion coefficient THD of 0.19 for one unit to approximately 3 %, is increased.

### B. Design of the Amplitude Detector from the Structure of the Digital Frequency Demodulator

The amplitude detector from the structure of the digital frequency demodulator was designed in the same way as the digital frequency modulator.

The amplitude detector was designed as follows [3]:  $U_{RL1} = 3.7$  V is accepted for logical 1 and  $U_{RL2} = 1.8$  V is accepted for logical 0 for the reference levels ( $R_L$ ) defining the hysteresis of Schmitt-trigger. Its width is obtained  $U_X = U_{RL1} - U_{RL2} = 1.9$  V. With a selected value of  $R_{13} = 10$  k $\Omega$  in equations (11) is compiled a system of two equations with two unknown quantities from which we can determine the resistance of resistors  $R_{15} 2948 \Omega$  and  $R_{14} 4396 \Omega$ . Their default values are chosen as 3 k $\Omega$  and 4.3 k $\Omega$ , respectively (Figure 9).

$$U_{RL1} = \frac{R_{14}}{R_{14} + R_{13}} \cdot U_{CC}; U_{RL2} = \frac{R_{14} \parallel R_{15}}{R_{13} + R_{14} \parallel R_{15}} \cdot U_{CC} \quad (11)$$

Since the designed FSK demodulator can be simulated only in the structure of the synthesized FSK modulator-demodulator (Figure 2) and thus Figure 9 presents the circuit for its simulation study. It also contains the FSK modulator (U1), two units of BPAF (U2, U3) and amplitude detector (U4).

The oscillogram of signals in nodes 2 (FSK modulated signal) and 3 - after both band-pass units, are shown in Figure 10. The latter appears to be the input for the FSK

demodulator (U4). The obtained oscillogram of the signals in nodes 2 (FSK modulated signal) and 4 - after the FSK demodulator is presented in Figure 11.

Since the output signal of the comparator of the FSK demodulator continuously switches with the frequency of the amplitude demodulated signal with the greater amplitude (Figure 11) available at logic 1 of the input modulation signal its rectification is required. For this purpose, the structure of the FSK demodulator envisages the use of a full-wave rectifier  $D_1$  (Graetz circuit) and a pulsating

smoothing capacitor  $C_8$ , in which case both intermediate signals of different amplitude are rectified – Figure 12.

The complete schematic circuit of the synthesized FSK modulator-demodulator containing Graetz rectifier and an inverter (U5) at the output of the FSK demodulator since the output signal is dephased at approximately  $180^\circ$  is shown in Figure 12.

The obtained oscillogram of the FSK modulated signal (node 2) and the rectified node 4 after Graetz rectifier (Figure 12) is shown in Figure 13.

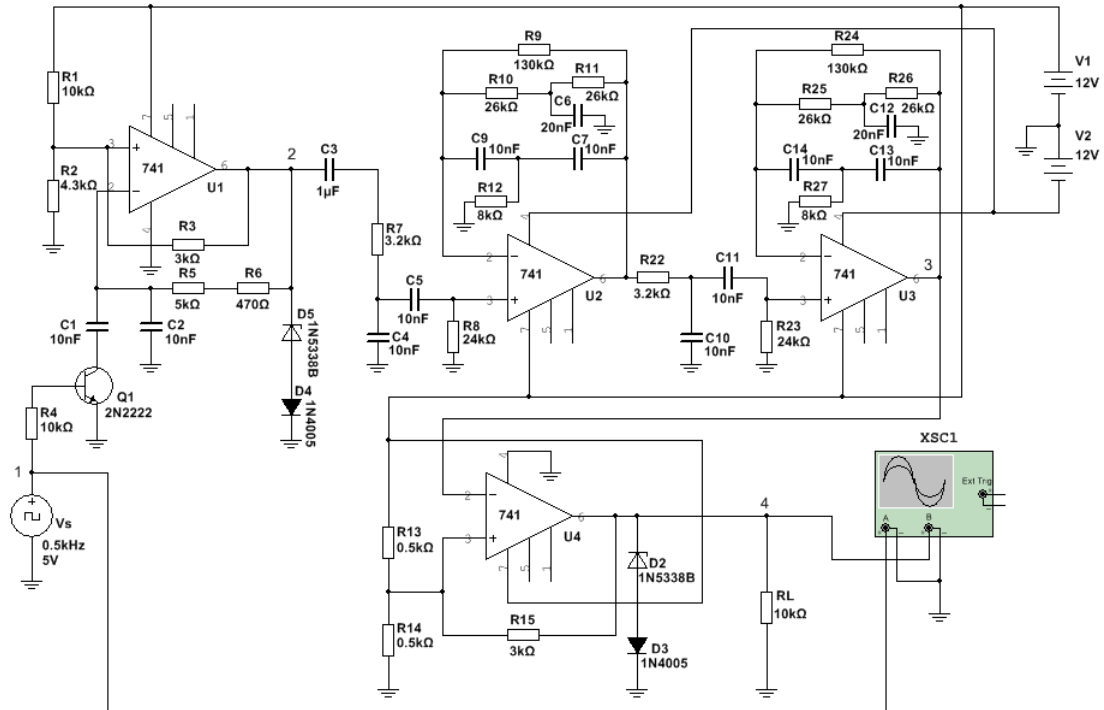


Figure 9: Circuit for simulation study of the synthesized FSK modulator-demodulator

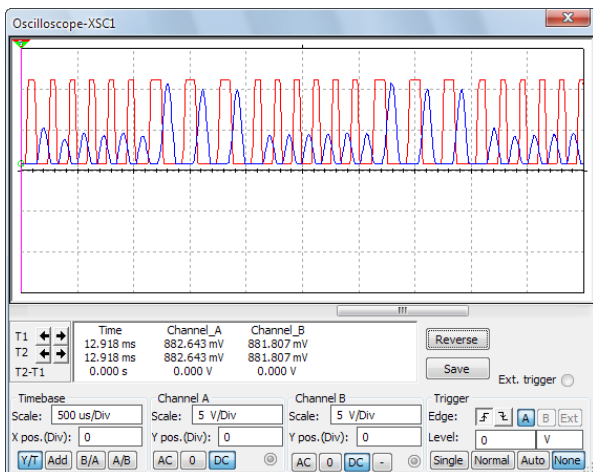


Figure 10: Oscillogram of the FSK modulated signal (node 2) and filtered after the two series connected BPAF (node 3)

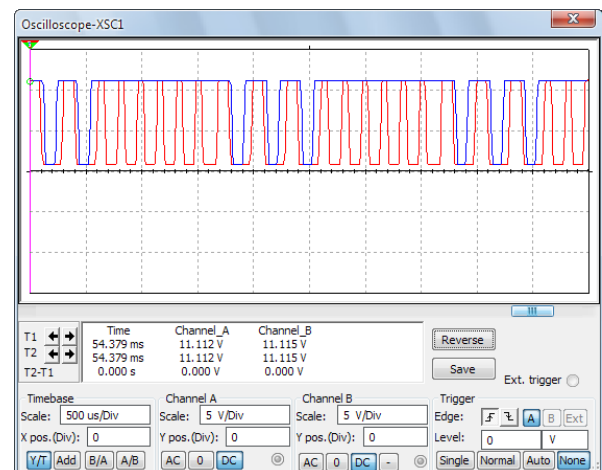


Figure 11: Oscillogram at the input and output of the synthesized FSK modulator-demodulator

The presence of a Graetz rectifier circuit in the FSK demodulator structure changes the DC signal levels for frequencies  $f_0$  and  $f_1$ . In this case, the reference levels defining the hysteresis of Schmitt-trigger for the FSK demodulator assume values  $U_{RL1} = 6.5 \text{ V}$  for logic 1 and  $U_{RL2} = 5.5 \text{ V}$  for logic 0. This requires a recalculation of the values of elements  $R_{13}$ ,  $R_{14}$  and  $R_{15}$  (Figure 12), as a result of which the value of hysteresis  $U_x$  is changed. At the selected value of  $R_{13} = 500 \Omega$  in equations (11), after solving the

system of two equations with two unknowns, the resistances of resistors  $R_{14} = 490 \Omega$  and  $R_{15} = 3096 \Omega$  are determined. For their standard values  $500 \Omega$  and  $3 \text{ k}\Omega$  are selected, respectively.

The simulated oscillogram at the input and output of the synthesized FSK modulator-demodulator (Figure 12) is shown in Figure 14.

The inverter (U5) in Figure 12 has  $A_U = R_{16}/R_{17} = 1$  and the values of the resistors are selected  $10 \text{ k}\Omega$  each. The values of  $R_{18}$  and  $R_{19}$  are determined by the required DC potential of the non-inverting input of the OA U5  $2.88 \text{ V}$ . With chosen value of the resistor  $R_{18} = 12 \text{ k}\Omega$  by dependence (12) for the value of  $R_{19}$  is obtained  $3899 \Omega$  as its default value is  $R_{19} = 3.8 \text{ k}\Omega$ .

$$U_{U5+} = \frac{R_{19}}{R_{18} + R_{19}} \cdot U_{CC}; 2.88 = \frac{R_{19}}{12 \cdot 10^3 + R_{19}} \cdot 12 \cdot (12) \quad (12)$$

The output signal of the modulator-demodulator has been dephased since both FSK modulator operating frequencies are larger than the center of the BPAF  $f_C = 1 \text{ kHz}$ . In this case, the right slope of the filter AFR is used. The output inverter (U5) will not be needed when using the left slope of the AFR of the BPAF.

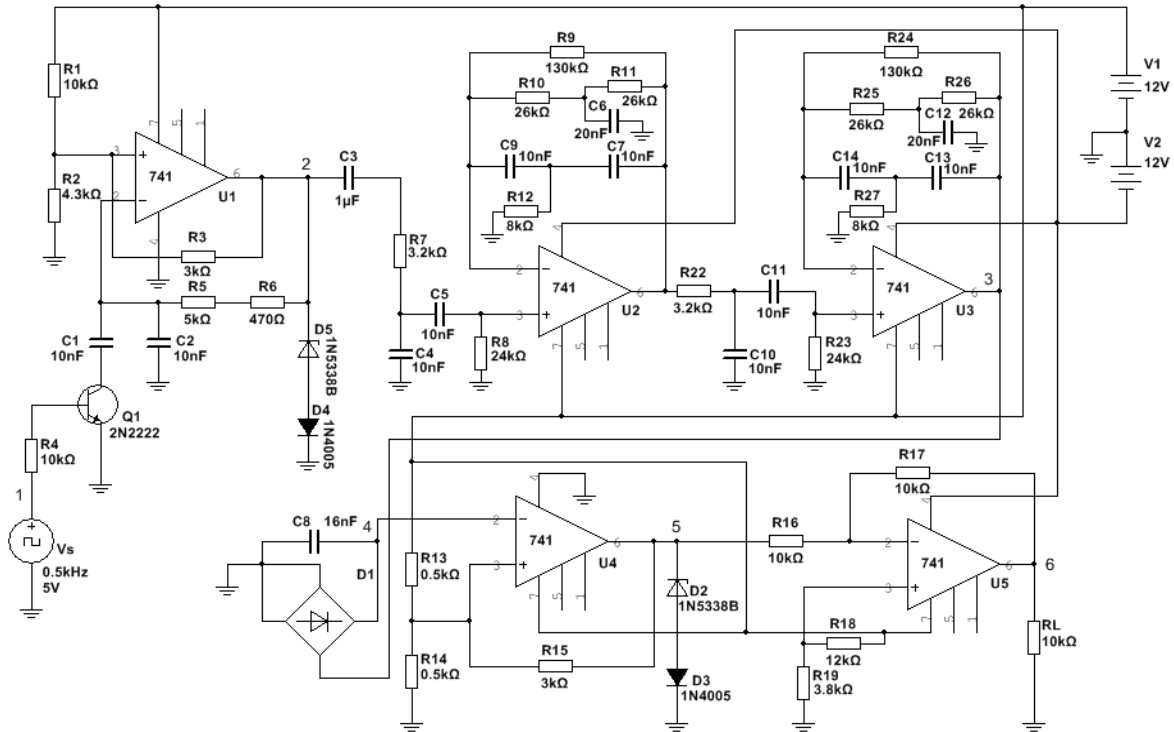


Figure 12: The complete circuit of the synthesized FSK modulator-demodulator

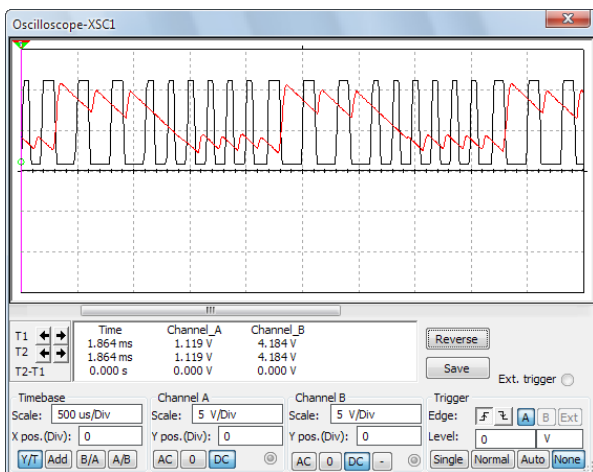


Figure 13: Oscillogram of the FSK modulated signal (node 2, black color) and the rectified node 4 (red color, Figure 12) after Graetz circuit

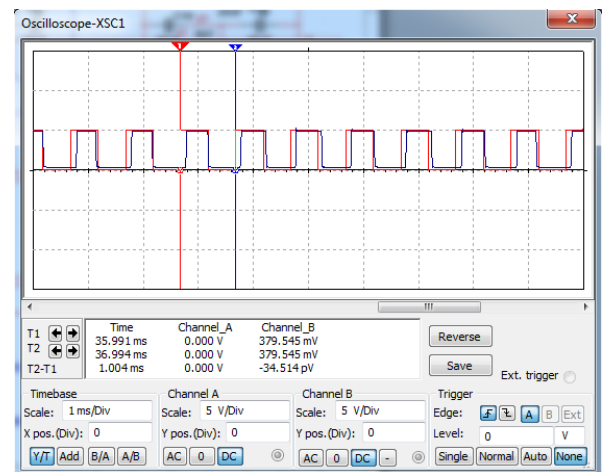


Figure 14: Oscillogram of the input (red color) and output (blue color) signals of the synthesized FSK modulator-demodulator

IV. EXPERIMENTAL STUDIES OF THE BAND-PASS ACTIVE FILTER AND SYNTHESIZED AND DESIGNED DIGITAL FREQUENCY MODULATOR-DEMODULATOR

A. Experimental Studies of the One and Two Units of Band-pass Active Filter from the Structure of the Digital Frequency Demodulator

The experimental studies have been carried out to establish the parameters and characteristics as well as the difference in the use of one and two units of BPAF from the FSK demodulator structure. The filters are implemented using an experimental suite Analog Experimenter TYPE 3205.

The experimentally obtained AFR and amplitude performances (AP) of the one and two units of BPAF are presented in Figures 15-16 (in normalized type) and Figures 17-18 respectively.

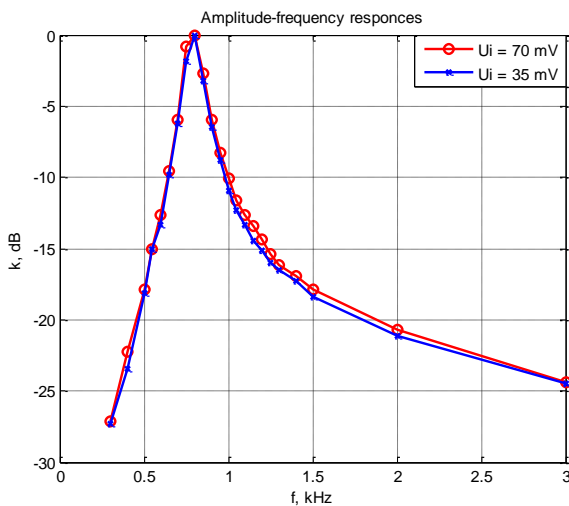


Figure 15: AFR of one unit of BPAF in normalized type

The main parameters of the practically implemented circuits of one and two units of BPAF are presented in Table 1.

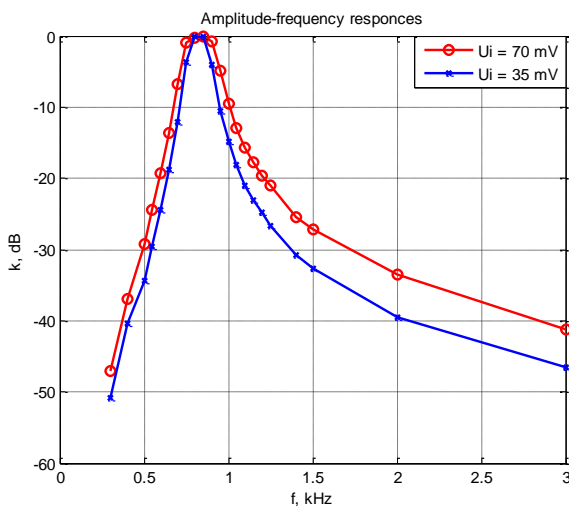


Figure 16: AFR of two units of BPAF in normalized type

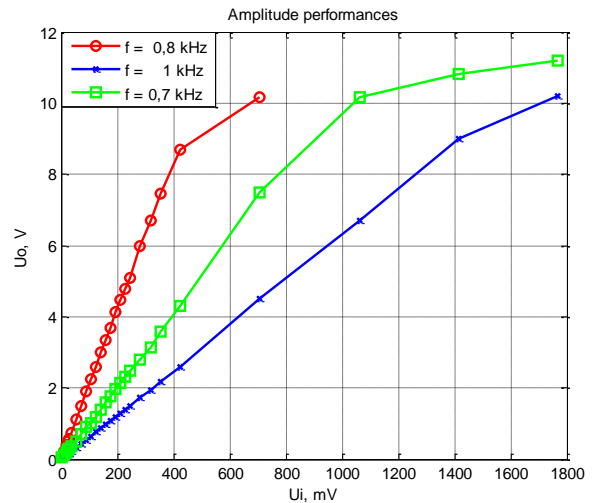


Figure 17: AP of one unit of BPAF

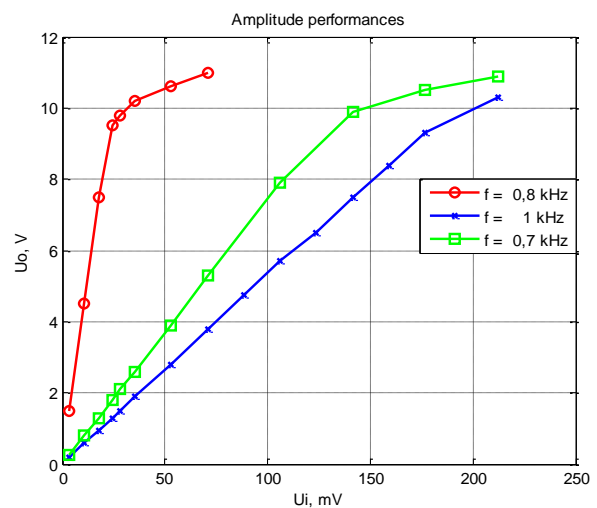


Figure 18: AP of BPAF with two units

Table 1  
The main Parameters of the Practically Implemented Circuits of One and Two Units of BPAF

Parameters of BPAF	with one unit	with two units
$f_c$ - a center frequency, kHz	0.8	0.85
$T_0$ - a maximum gain for the $f_c$	21.14	297
$f_b$ - bellow- cut-off frequency, kHz	0.72	0.72
$f_h$ - high- cut-off frequency, kHz	0.82	0.94
$\Delta f$ - pass bandwidth, kHz	0.10	0.22
$u_{i\min}$ , mV ( $f=0,8$ kHz)	10	10
$u_{i\max}$ , mV ( $f=0,8$ kHz)	424.3	24.7
$D$ - dynamic range ( $f=0,8$ kHz)	42.43	2.47

From the presented characteristics (Figures 15 - 18) and parameters (Table I) of the one and two units of BPAF from the FSK demodulator structure, which has been implemented and studied separately, it is established that:

- the center frequency at both input voltages is the same;
- the selectivity of the BPAF at the lower input voltage value  $u_i = 35$  mV (Figure 16) is greater, and the pass bandwidth is narrower;
- the transmission coefficient for the center frequency  $T_0$  increases by about 15 times when connecting the two band-pass units sequentially, which leads to a

slight increase in the bandwidth. There is also a miniaturized center frequency shift of 50 Hz;

- the gain coefficient is the highest at the center frequency as well as at the angle that the corresponding characteristics make with the  $U_i$  axis (Figures 17 and 18), with the smallest dynamic range realized. The AP have a large linearity of the gain in the corresponding limits of dynamic range.

**B. Experimental Studies of the Synthesized Digital Frequency Modulator-demodulator**

A complete technical documentation has been developed using UltiBOARD module of Circuit Design Suite package. The type of the printed circuit board is presented in Figure 19 (assembled design) and the 3D model of the developed digital frequency modulator-demodulator in Figure 20. A laboratory model of the synthesized and designed digital frequency modulator-demodulator (Figure 12) has been implemented, which has also been studied experimentally.

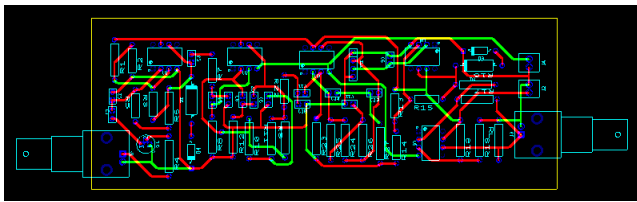


Figure 19: The type of the printed developed circuit board

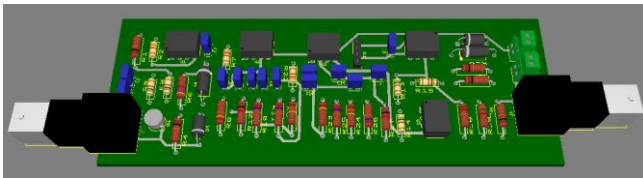


Figure 20: 3D model of the developed digital frequency modulator-demodulator

The experimentally obtained oscillograms in the specified nodes of the synthesized and implemented circuit of a digital frequency modulator-demodulator (Figure 12) are shown in Figures 21 - 26 [11]. A generator is connected to the input of the circuit, as the applied signal is bipolar with rectangular pulses with amplitude from peak to peak  $U_{PP}$  5 V, frequency 500 Hz and 50 % duty cycle.

The oscillogram of the input modulation signal supplied by the set generator - bipolar symmetric rectangular pulses with the amplitude  $U_{PP}$  of 5 V and a frequency of 500 Hz is shown in Figure 21. The type of signal fed to the input of the FSK modulator (node 2 of the OA U1) with amplitude  $\Delta Y = 1.86$  V and frequencies  $f_1 = 3.79$  kHz,  $f_0 = 6.58$  kHz respectively for logic 1 and logic 0 is presented in Figure 22. Its shape is triangular with a pronounced increasing forward front, with minimal parasitic amplitude modulation when frequency varies.

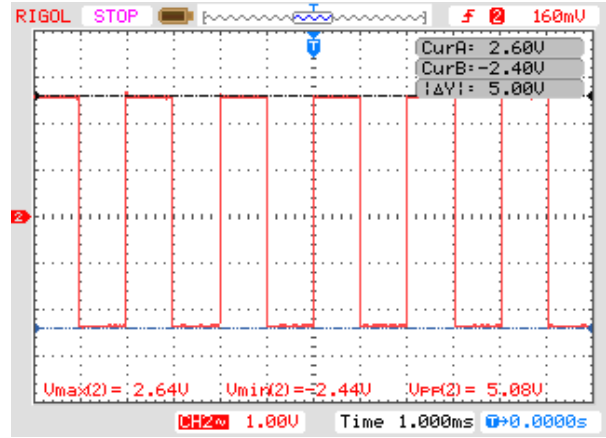


Figure 21: Oscillogram at the input digital modulation signal - node 1

The obtained oscillogram at the output of the FSK modulator (node 6 of the OA U1) is presented in Figure 23 as rectangular pulses with the same amplitude and the same frequencies  $f_1 = 3.79$  kHz,  $f_0 = 6.58$  kHz respectively for logic 1 and logic 0.

The types of signals for the two operating frequencies  $f_1 = 3.79$  kHz and  $f_0 = 6.58$  kHz after the filtration of the first BPAF (BPAF1) - node 6 of the OA U2 are shown on the oscillogram in Figure 24.

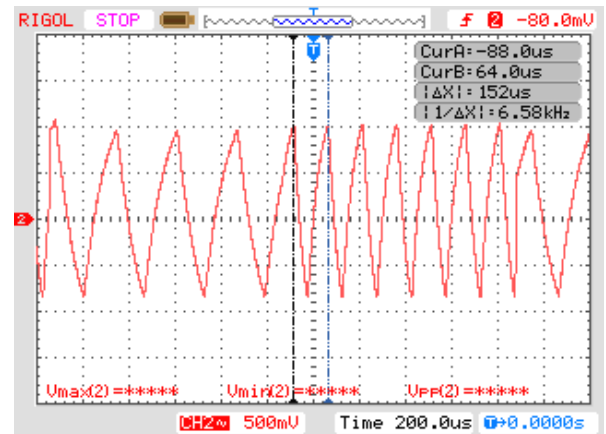


Figure 22: Oscillogram at the input of FSK modulator at logical 0 with  $f_0 = 6.58$  kHz - node 2 of OA U1

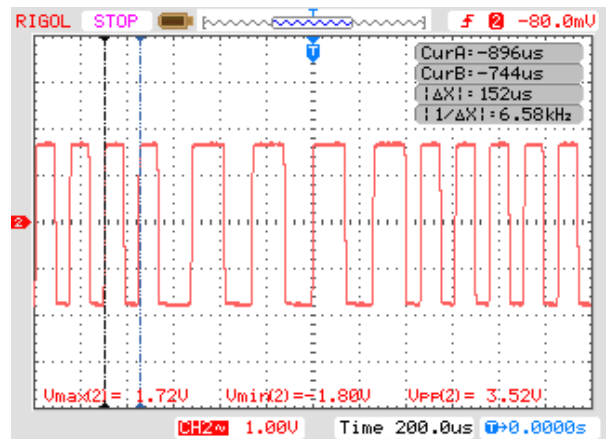


Figure 23: Oscillogram at the output of the FSK modulator with  $f_0 = 6.58$  kHz - node 6 of OA U1

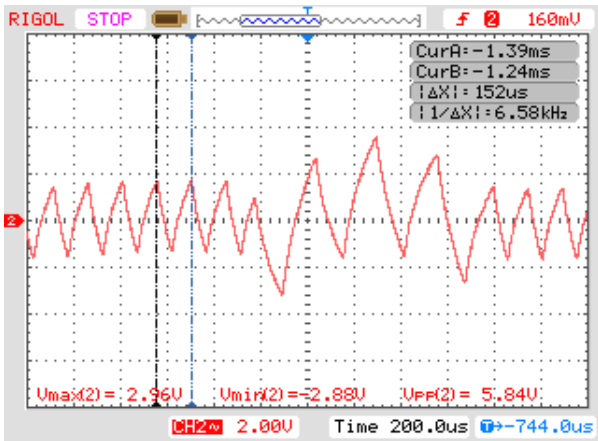


Figure 24: Oscillogram at the output of the BPAF1 ( $f_0=6.58$  kHz) - node 6 of OA U2

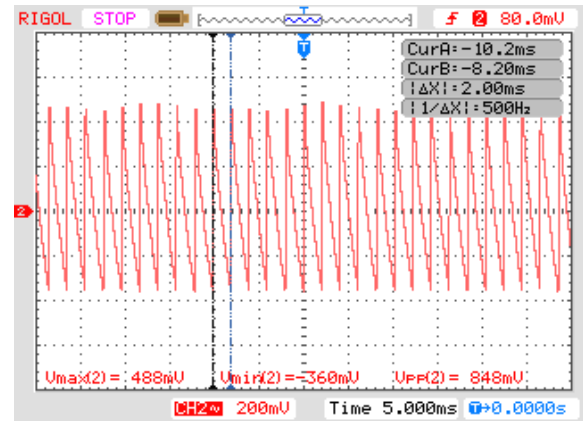


Figure 26: Oscillogram at the OA U4 input - node 2

The oscillogram of the output of BPAF2 (node 6 of OA U3) for the two operating frequencies is shown in Figure 25. It shows a minimum change in pulse width and a slight decrease in the frequency of the lower operating frequency. At the higher operating frequency ( $f_0 = 6.58$  kHz), a symmetrical and mirror change in amplitude of the pulses within the respective half-period is observed - the pulses change their polarity and their shape changes mirror-like.

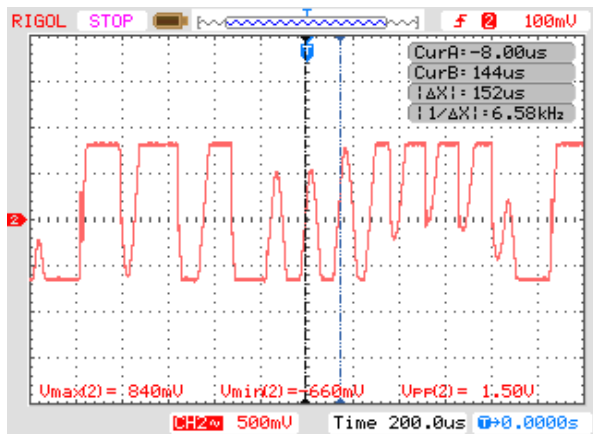


Figure 25: Oscillogram at the output of the BPAF2 - node 6 of OA U3 ( $f_0=6.58$  kHz)

The signal type, after the Graetz rectifier circuit and at the input of OA U4 (node 2), is shown on the oscillogram in Figure 26. It is characterized by minimal amplitude variation, has the frequency of the input modulation signal  $f = 500$  Hz and a well-pronounced rear front. After passing through the amplitude detector (OA U4) and the inverter (OA U5), the type of oscillogram of the output signal with regard to the input modulating one, is analogous to that shown in the simulation studies - Figure 14.

## V. CONCLUSION

The synthesis of a digital frequency modulator-demodulator is related to the development of a conceptual design in which the requirements for the individual component blocks and the possibilities for their choice and implementation were presented. The design, simulation, and experimental study of a digital frequency modulator with a timer-module 555 and a Schmitt-trigger have been carried out.

Among the choices of FSK demodulator - coherent, differential-coherent and non-coherent - the latter was chosen because its implementation is not related to the use of specialized integrated circuits such as PLL and DSP. It was synthesized by BPAF: two second order units and an amplitude detector (Schmitt-trigger comparator). The simulation and experimental studies were performed for all composite modules as well as for the entire synthesized non-coherent digital frequency modulator-demodulator by presenting the results obtained by visualising the processes in progress.

The methodology of the development of the FSK modulator-demodulator includes conceptual design and the use of numerical, simulation and experimental approaches. The numerical approach is used in the design of the individual blocks of the non-coherent FSK demodulator as well as in the determination of the values of the selected circuit variant elements. The simulation approach provides an evaluation of the qualitative parameters of the separate FSK modulator-demodulator blocks, as well as the optimization of the values of the elements of the designed circuit variants. The experimental approach was applied to the study of the developed laboratory model of the FSK modulator-demodulator. On the basis of the obtained results, assessment was made and was compared to the results obtained from the simulation study. Because the simulation and experimental results obtained are similar, it has been established that the carried out synthesis, design and modeling of the non-coherent FSK demodulator was successful.

This paper presents a synthesized, modeled and implemented schematic variant of a digital modulator-demodulator with the use of analogue linear and non-linear circuits with operational amplifiers.

REFERENCES

- [1] D. Dobrev, L. Yordanova, "Radiocommunications", parts one and two, Publishing house SIELA, Sofia, respectively 2001 and 2003.
- [2] I. Nemigenchev and B. Karapenev, "Communication Transform Devices", University Publishing House "Vasil Aprilov", ISBN 978-954-683-361-7, Gabrovo, 2007.
- [3] B. Karapenev, "Synthesis and Study of Digital Frequency Modulator-Demodulator". Journal of Communications Technology, Electronics and Computer Science. Issue 13, pp. 1-9, 2017. ISSN 2457-905X. DOI: <http://dx.doi.org/10.22385/jctecs.v13i0.218>. The prefix of the journal is 10.22385. <http://jctecs.com/index.php/com/issue/archive>
- [4] B. Song, In Lee, "A digital FM demodulator for FM, TV, and wireless", IEEE Transactions on Circuits and Systems II: Analog and Digital Signal Processing, volume: 42, issue: 12, pp. 821-825, Dec 1995.
- [5] A. Parasar, M. Kimothi, "Design implementation of digital FM modulator & demodulator for SDR using FPGA", International Journal of Engineering Sciences & Research Technology, ISSN: 2277-9655, pp. 178-186, March 2018.
- [6] B. Karapenev, "Macromodel synthesis of digital non-coherent frequency demodulator and simulation studies of FSK modulator-demodulator", Journal of the Technical University of Gabrovo, volume 54, ISSN 1310-6686, pp. 45-48, 2017.
- [7] Thierry Taxis, Hassène Kraïmia, Didier Belot and Yann Deval, "An FSK and OOK Compatible RF Demodulator for Wake Up Receivers", Journal of Low Power Electronics and Applications, ISSN 2079-9268, pp. 276-277, November 2015, [www.mdpi.com/journal/jlpea](http://www.mdpi.com/journal/jlpea)
- [8] St. Koutsarov, "Electronic circuit manual", part V, Electronic filters, Sofia, Technika Publishing house, 1982.
- [9] B. Karapenev, "A digital frequency modulator using module-timer 555", Scientific papers at the University of Rousse, Volume 54, Series 3.2, ISSN 1311-3321, pp. 41-46, 2015, <http://conf.uni-rouse.bg/bg/docs/cp15/3.2/3.2-6.pdf>
- [10] B. Karapenev, "A digital frequency modulator using Schmitt-trigger", Scientific papers at the University of Rousse, Volume 54, Series 3.2, ISSN 1311-3321, pp. 92-98, 2015, <http://conf.uni-rouse.bg/bg/docs/cp15/3.2/3.2-14.pdf>
- [11] B. Karapenev, "Studies of Synthesized and Implemented Digital Frequency Modulator-Demodulator", ITHEA, International Journal "Information Theories & Applications", Volume 25, Number 3, 2018, ISSN 1310-0513 (printed), 1313-0463 (online). pp. 289-299.